BNL 29465
CONF-810246--3

MASTER

Highlights of High Energy pp, $\bar{p}p$ and e^+e^- Interactions*

Ling-Lie Chau Wang
Physics Department
Brookhaven National Laboratory
Upton, New York 11973

April

The submitted manuscript has been authored under contract DE-AC02-76CH00016 with the U.S. Department of Energy. Accordingly, the U.S. Government retains a nonexclusive, royalty-free license to publish or reproduce the published form of this contribution, or allow others to do so, for U.S. Government purposes.

*This talk was presented at the Cornell "Z^0-Physics" Workshop, February 6-8, 1981.

Highlights of High Energy pp, $\bar{p}p$ and e^+e^- Interactions

Ling-Lie Chau Wang

Contents

*This talk was presented at the Cornell "Z^{o}-Physics" Workshop, February 6-8, 1981.

I. INTRODUCTION

We are certainly living in an unprecedented era in the history of physics. With a single parameter $\sin^2\theta_w = .23 \pm 0.02$ the electroweak unified theory[1] of SU(2) x U(1) has succeeded in fitting many different categories of weak interaction data.[2] In cooperating strong interaction, the scheme of grand unification theory,[3] GUT, permits the proton to be unstable.[4] From this single parameter and the renormalizability of GUT, the masses of the intermediate bosons are precisely predicted,[5] $M_Z = 80$ GeV, $M_W = 90$ GeV. The exciting fact is that they are within the production and detection of the near future high energy pp, $\bar{p}p$ and e^+e^- machines. The 50 GeV on 50 GeV e^+e^- machine under study here is certainly valuable for the search of the Z^o boson and the subsequent production of the Higgs boson and new flavors.

Since the production of Z^o and its subsequent decay properties into leptons was thoroughly reported in the previous Cornell[6] and LEP[7] studies, I shall report in more detail a recent update of the study in pp and $\bar{p}p$ interaction.[8] Comparisons of production rates between pp, $\bar{p}p$ and e^+e^- machines are given, see Table I and the Summary in this report.

II. pp, $\bar{p}p$ INTERACTIONS

(A) ESTIMATING THE PRODUCTION CROSS-SECTIONS OF $W^{\pm}$, Z^o

The production cross section of $W^{\pm}$, Z^o can be estimated from current measurements of virtual photon production in the inclusive dilepton production of nucleon-nucleon reactions utilizing the result of CVC and the conjecture of scaling. CVC tells us that the production cross section[9] of $W^{\pm}$ of mass m_w is related to that of the virtual photon at the same invariant mass $Q = m_w$ by

$$\sigma_w \gtrsim \frac{4}{3}\frac{G}{2\alpha^2} Q^3 \frac{d\sigma}{dQ} \simeq (0.1\ \text{GeV}^{-2})\ Q^3 \frac{d\sigma}{dQ}. \qquad (2.1)$$

However, the current experiments limited by the current machine energy give us $d\sigma/dQ$ only up to $Q \simeq 20$ GeV. In order to obtain $d\sigma/dQ$ at higher Q at higher energies, we need to use the hypoth-

esis of scaling, i.e. the dimensionless cross section $Q^3\, d\sigma/dQ$ is a function of the dimensionless variable Q^2/s, where $\sqrt{s}$ is the center of mass energy,

$$Q^3 \frac{d\sigma}{dQ} = f(Q^2/s). \tag{2.2}$$

Thus the production of higher mass Q at corresponding higher energy s can be predicted from low energy data. In Fig. (2.1a) the compilation of data[10] including the latest CERN data of Becker et al[11] at $\sqrt{s} = 62$ GeV, for $Q^3 \frac{d\sigma}{dQ}$ are plotted in scaling variables s/Q^2, with 8 GeV < s < 62 GeV and 2 GeV < Q < 10 GeV. Also shown in Fig. (2.1b) are the collection of data[12] for $Q^3\, d\sigma/dQdy \,|_{y=0} = \sqrt{4Q^2/s}\, d\sigma/dQdx \,|_{x=0}$, which is also a scaling cross section in the scaling variable $Q/\sqrt{s}$, where $y = \ln (E-p_\ell^*)/(E + p_\ell^*)$, where E and p_ℓ^* are the energy and longitudinal momentum of the virtual photon. Considering the range of energies and masses involved, scaling works very well.

In 1970, Drell-Yan[13] proposed a model in which the production of virtual photon is from the annihilation of a quark q and an anti-quark $\bar{q}$ from the two interacting hadrons, which in turn is directly related to the lepton hadron inclusive reactions, as shown in Fig. (2.2a), Fig. (2.2b). The scaling hypothesis of Eq. (2.2) is naturally related to the approximate scaling phenomenon observed in lepton-hadron inclusive reactions. The result of CVC can now be specifically incorporated in the elementary interactions of $q\bar{q} \to \gamma_v$, $W^{\pm}$, $Z^0 \to \ell\bar{\ell}$. Thus given the structure functions from lepton-hadron inclusive reactions, the $W^{\pm}$, Z^0 production can be calculated.

First a few words about the development of our knowledge of the quark structure functions. In 1969, Bjorken and Feynmann[14] conjectured that the structure function in e p inelastic scattering $\nu W_2 = F_2$, which is in general a function of the virtual photon mass $q^2 = -Q^2$ and the total invariant energy $2m\nu$, is a function of the dimensionless variable $2m\nu/Q^2 = x$, which denotes the fractional momentum of the proton the quark carries. Later this

approximate scaling is considered to be a consequence of asymptotic freedom[15] in the framework of QCD for the hadrons. Due to this property of asymptotic freedom, a perturbative calculation scheme can be formulated to analyze quantitatively the change of structure function as Q varies. In the leading-log approximation to all orders of α_g, it amounts to the calculation of sum of all ladder diagrams as shown in Fig. (2.3b). The variation in Q^2 for fixed x, or violation of scaling, is found to be logorithmic and most severe in the small x region $x \lesssim .1$ and small Q^2 region $Q^2 \lesssim 100\ GeV^2$ as shown in Fig. (2.4a) and (2.4b), taken from Ref. (16). In this approximation, the structure functions used for Drell-Yan are still those directly obtained from lepton-hadron reactions including their scaling violation effects, see Fig. (2.3). In Fig. (2.1a) we plot the dilepton cross sections $Q^3\ d\sigma/dQ$ obtained from such a calculation. We see that actually the predicted cross sections (dashed curves) using currently available structure functions including scaling violation effects, agree with the data much better than the old prediction (solid curve) using the then (up to 1977) available low-Q^2 structure functions from lepton-hadron inelastic scatterings.

Thus far the gross features predicted by perturbative QCD have been born out in the lepton-hadron inclusive reactions. However, there are still many details needed to be checked out, notably the systematic inconsistent implications on the running coupling constant α_g from μp and νp in elastic scattering.[17] As for the virtual photon production in hadron-hadron reactions, the next order QCD calculation, i.e. consider in Fig. (2.3a) one additional gluon emission in all possible ways, is causing trouble. It is found that the correction term is as big as the original one.[18] This difficulty can not be settled until higher order terms are calculated. For our purpose of estimating $W^{\pm}$, Z^o productions, we shall use the Drell-Yan scheme as shown in Figs. (2.3a) and (2.3b), i.e. ignoring the higher order QCD corrections beyond the leading-log.

Using the general calculational scheme of Ref. (19), and the quark structure functions fitting the durrent lepton-hadron inelastic cross section,[20] and the recent updating work of Ref. (21), we shall present many results of the $W^{\pm}$, Z^{o} production and their decay products.

Figs. (2.5a) (2.5b) shows the production cross sections of $W^{\pm}$ and Z^{o}, $Sin^{2}\theta_{w} = .22$, $m_{w} = 80$ GeV and $m_{z} = 90$ GeV at varied energies. We plotted the cross section vs $\sqrt{s}/m$, therefore the curves can also be read off for productions of $W^{\pm}$ and Z^{o} at other values of masses and energies, with the Fermi coupling constant G being kept the same. From Figs. (2.5a) and (2.5b) we see that there will be about 5×10^{7} $W^{\pm}$, Z^{o} produced per year ($\sim 3 \times 10^{7}$ sec) at ISA. For comparison the production of $W^{\pm}$ and Z^{o} in $p\bar{p}$ and the yield at the future $p\bar{p}$ machines ($\sqrt{s}$ = 540 GeV at CERN, and $\sqrt{s}$ = 2000 GeV at Fermilab, luminosity 10^{30} cm^{-2} sec^{-1}) are also given. The high luminosity at ISA is certainly a great advantage.

(B) THE DETECTION OF THE Z^{o} AND W^{+}

The Z^{o} and $W^{\pm}$ need to be detected via their decay products.

1. Leptonic Decay

Here we estimate the branching ratio by counting the decay channels of leptons and quarks. The $W^{\pm}$ coupling to all leptons and quarks are equal, the (V-A) coupling, thus the leptonic branching ratio is

$$B(W\to\ell\bar{\nu}_{\ell}) = (W\to\ell\bar{\nu}_{\ell}) \,/\, (W\to\ell\bar{\nu}_{\ell},\ \mu\bar{\nu}_{\mu},\ \tau\bar{\nu}_{\tau},\ \sum_{i=1}^{3} u_i\bar{d}_i,\ \sum_{i=1}^{3} c_i\bar{s}_i,\ \sum_{i=1}^{3} t_i\bar{b}_i) = 1/(1+1+1+3+3+3) = 1/12, \tag{2.3}$$

where the sum over i is the SU(3) color index sum. For Z^{o}, its vector and axial couplings to the leptons and quarks are $C_{v,j} = 2\,(I_{z,j} - 2Q_j Sin^{2}\theta_{w})$, $C_{a,j} = -\sqrt{2}$, where j denotes lepton or quark type, Q_j and $I_{z,j}$ denotes the charge and the third component of the isospin respectively. Note that for $Sin^{2}\theta_{w} = .23$, the vector

coupling for e^-, μ^-, τ^- are very small, and also that

$$B(Z^0 \to \ell\bar{\ell}) = (C_{v,\ell}^2 + C_{a,\ell}^2) / \sum_j (C_{v,j}^2 + C_{a,j}^2) \approx 3\% , \qquad (3.2)$$

Fig. (2.6) shows the cross section $d\sigma/dQdy\big|_{y=0}$ of pp (or $p\bar{p}$)$\to Z^0X \to \ell\bar{\ell}X$ which has a peak around the Z^0 mass, with a half width of 1.25 GeV and Fig. (2.7) shows the single lepton production cross section $d\sigma/dp\ d\Omega$ of $PP \to W^{\pm}X \to \ell^{\pm}(\nu X)$, which a sharp decline around $P = \frac{1}{2}m_W$. The figures also give the rate for the given machine luminosity. We see that, with the high luminosity of ISA, the $Z^0 \to \ell\bar{\ell}$ and $W^{\pm} \to \ell^{\pm}\nu$ are plentifully produced. We see from Figs. (2.5), (2.6), (2.7) that using 300 events/year as a criteria, $W^{\pm}$ or Z^0 with masses up to 300 GeV can be observed at ISA.

2. Hadronic Decay of $W^{\pm}$ and Z^0

The $q\bar{q}$ decay product of $W^{\pm}$ and Z^0 will become hadronic jets like those observed in e^+e^- reactions. However, their cross sections are way below those from pure hadronic cross sections, see Fig. (2.8). Thus it is not a viable method to look for $W^{\pm}$ and Z^0 by their hadronic decays unless some further triggering means are used.[22]

(C) Some Detail Features of the Drell-Yan Model

Due to the (V-A) coupling nature of the $W^{\pm}$, the coupled quarks and leptons have left-handed helicity, and the coupled anti-quarks and anti-leptons have right-handed helicity. In the Drell-Yan model, (ignoring the $p_\perp$ motion of the quark), the $q,\bar{q}$ system, annihilating collinearly to become $W^{\pm}$, had total helicity one pointing in the p direction. Therefore the $W^{\pm}$ produced are polarized and its decay product $\ell,\bar{\ell}$ will remember this polarization. The right-handed $\bar{\ell}$ will move in the $\bar{q}$ direction, and the left handed ℓ will move in the quark direction. So the longitudinal motion of ℓ will reflect that of the q and $\bar{\ell}$ that of $\bar{q}$.

As shown in Fig. (2.8), for $P_\perp < \frac{1}{2}m_W$ $\ell^-(\ell^+)$ from $W^-(W^+)$ produced in $p\bar{p}$ peaks strongly in the $p(\bar{p})$ direction reflecting the $u(\bar{u})$ quark motion in the proton (antiproton) direction. However, it is interesting to note that as $P_\perp \approx \frac{1}{2}m_W$, the $\ell^+(\ell^-)$ has only the longitudinal motion totally from $W^+(W^-)$, which is produced moving preferably in the $p(\bar{p})$ direction; thus $\ell^+(\ell^-)$ now moves in the $p(\bar{p})$ direction. For p,p scaling the distribution is forward-backward symmetry. Fig. (2.9a)and (2.9b) show that ℓ^- longitudinal motion reflects the valence quark distribution, which is more forward-backward peaked, and the ℓ^+ reflects the sea quark momentum distribution which is more central peaked. In Fig. (2.9c) and (2.9d) $P_\perp \approx m_W$, $\ell^+(\ell^-)$ is forced to move in the direction of $W^+(W^-)$. The m_W distributions reflect the difference in the $W^+(W^-)$ production. Since W^+ is produced from $u\bar{d}$, W^- from $d\bar{u}$, the former has a larger cross section. With a value $\sin^2\theta_W \approx .23$, the coupling of Z^o to $\ell\bar{\ell}$ is almost completely axial, see Eq. (2.3), the effects mentioned above will be almost absent for the $\ell\bar{\ell}$ from Z^o decay.

One may also ask if there are other parity violation effects e.g. the asymmetry in $\vec{p}_{lep}$ distribution reflected on the opposite side of the $(p_{\perp,W} \times p_{beam})$ plane. Though the coupling is (V-A), maximal parity violation, the Drell-Yan model does not give such asymmetry due to the fact that the Drell-Yan amplitudes are real.[23] This will be another detail test of the model.

(D) ESTIMATE OF ONIA PRODUCTION

It was proposed by Gaisser et al,[24] that the cross section $(\Gamma_h)^{-1}m^3\frac{d\sigma}{dx}$ for massive meson production is a scaling function of $\sqrt{s}/m$ and x only, i.e. $(\Gamma_h)^{-1}m^3\frac{d\sigma}{dx} = f(s/m^2, x)$, where $x = p_\ell^*/\frac{1}{2}\sqrt{s}$, m is the mass of the meson, and Γ_h is the partial width of the meson decaying into ordinary hadrons. The conjecture is based on dimensional arguments and the division of Γ_h is intended to eliminate the onia type dependence in the production. In

Fig. (2.10a) taken from Ref. (25), the compilation of $\Gamma_h^{-1} m^3 \frac{d\sigma}{dy}\Big|_{y=0}$ $= \Gamma_h^{-1} m^3 \sqrt{4m^2/s} \frac{d\sigma}{dx}$, also a scaling function in $m/\sqrt{s}$, for the production of all heavy vector meson productions are given. Considering the great variation in $d\sigma/dy\,|_{y=0}$, see Fig. (2.10b) various m productions, the scaling is impressive. Though there is not justifiable reason for it, the exitation curve has a shape very close to that of $\ell\bar{\ell}$ from γ_v, or the Drell-Yan curve of Figs. (2.1). Using this curve of $f(s/m^2,x)$, the cross section multiplied by the leptonic branching ratio $B_{\ell\bar{\ell}} \equiv \Gamma(V\to\ell\bar{\ell})/\Gamma(V\to\text{all})$ can be obtained

$$B_{\ell\bar{\ell}} \frac{d\sigma}{dx} = B_{\ell\bar{\ell}} \frac{\Gamma_h}{m^3} f(s/m^2,x) = \frac{\Gamma(V\to\ell\bar{\ell})}{m^3} f(s/m^2,x), \qquad (4.1)$$

if $\Gamma(V\to\text{all}) = \Gamma_h$ and if we can estimate $\Gamma(V\to\ell\bar{\ell})$. Using potential models for large enough m, mass of the particle V, the effective potential becomes Coulombic and $\Gamma(V\to\ell\bar{\ell})\simeq m$. In order to make a conservative estimate, we shall use $\Gamma(V\to\ell\bar{\ell})$ = constant = $\Gamma(J\to\ell\bar{\ell})$. In Fig. (2.11) we show such a calculation by F. Paige[26] of heavy onia production together with that of γ_v and Z^o production. Note that the widths of the onia are totally from the assumed 1% resolution of experimental detection. Also note that the contour of the onia peaks follows that of the γ_v. This is a consequence followed directly from the fact mentioned before that the scaling curve $f(s/m, x)$ has the similar shape as that of γ_v production. Again if we use a limit of 300 events/year, onia of mass up to 120 GeV can be studied at ISA.

(E) HIGGS BOSON AND TECHNICOLOR PSEUDO SCALAR PRODUCTION

As we have discussed all along that the standard SU(2) x U(1) model has great phenomenological successes with its single parameter $\text{Sin}^2\theta_w = .23 \pm .02$, and provides definite information about the $W^{\pm}$ and Z^o masses. Here we have also given detailed information about their productions and detections in hadronic scatterings.

However, there is a corner of the model that is still quite obscure, i.e. how the mass-generation comes about. In the original form, the intermediate boson masses are generated by the fundamental scalar Higgs fields. Three of them are used up in mass-generating and a neutral Higgs boson H^0 is left as a physical particle. Though its coupling to the intermediate bosons and quarks are given by the model, its mass is completely unconstrained. Also ways to detect such boson have been noticeably missing in hadronic scattering, contrasting to the situation with e^+e^- machines for which signatures and ways to observe such boson are rather clear. Here I want to report a signature[28] of the H^0 production in hadronic scattering. We show that the bremsstrahlung of the H^0 by a Z^0 produced in hadronic scattering, see inset of Fig. (2.12) shows up as a bump in the dilepton mass Q distribution with a fast fall off at $Q = m_Z - m_H$. Using the same Drell-Yan model, Fig. (2.12) shows the calculated $d\sigma(s,Q)/dQ$ for the H^0 production for m_H = 5 GeV, 10 GeV, 15 GeV and 20 GeV at $\sqrt{s}$ = 800 GeV. We see that besides the peak at $Q = m_Z$, which comes from the Breit-Wigner (B-W) propagator of the outer Z^0, there is a bump with a sharp fall near $Q = m_Z - m_H$, which reflects the B-W propagator of the inner Z^0. The slow fall as Q decreases from $Q = m_Z - m_H$ comes again from the outer Z^0 propagator. In Fig. (2.13) we compare the Q distributions with and without the H^0 (m_H = 15 GeV) emission. We see that the peak at $Q = m_Z$ with H^0 emission is about three orders of magnitude below that without the H^0 emission. However, the second bump is enticingly not too far below the background of the γ_v and Z^0 productions. With the projected luminosity of ISABELLE 10^{33} cm^{-2} sec^{-1}, there will be about 600 events/year (3.15×10^7 sec) from the bump between 66 GeV < Q < 76 GeV in the case of $\sqrt{s}$ = 800 GeV and m_H = 15 GeV. As low as it is, however, it is not completely out of question to accumulate enough events for its detection in case we can eliminate the background above. To get rid of the background, we propose to trigger on a third lepton of a few GeV in

momentum beside the original two fast leptons with momentum = $\frac{1}{2}(m_Z - m_H)$, using the property that the H^o prefers to couple (with a strength m_f^2 G) to the most massive fermion pair allowed, i.e. $c\bar{c}$ or $\tau\bar{\tau}$, for $2m_\tau < m_H < 2m_b$, and $b\bar{b}$ for $2m_b < m_H < 2m_t$. c,τ have a 15% branching ratio decaying into a charged lepton, and the b has even higher portion of its final states having a lepton[29] due to its cascade decay into the charm. Thus by this trigger the bump is reduced less than 30%, however we anticipate the reduction much more for the background from our current understanding of single lepton productions.[30] If the Higgs masses are much bigger than $2m_b$, it may be also triggered by two hadronic jets. Such detail analysis shall be carried in the future.

Due to the smallness of the cross section, it definitely points to machines with high luminosity besides high energy. Note also that for small m_H, a detector of good mass resolution is needed, in case if the background of the single Z^o production can be triggered away. Since the mechanism discussed here is a kinematic one, similar effects exist for any emission of a massive particle by a resonance. Thus this phenomena provides a new means to discover new particles in the cases when the coupling strength of the emission is large enough. Further, the Higgs boson bremsstrahlung mechanism discussed here provides an explicit example that the detecting of the trilepton or dilepton plus jets might be the way for future experiments to discover new particles, in addition to the historically successful method of detecting the diplepton system.

Recently a new scenario is being proposed, the technicolor scheme, in which the fundamental Higgs field are replaced by dynamically generated Goldstone bosons.[31] This is a scheme borrowed from the phenomena in superconducting materials, the technicolor fermions $(U, D)_L$, U_R, D_R, (many of them) play the role of the electrons, the technicolor pseudo-scalars π'_i, η'_i, (many of them) correspond to the Cooper pairs. The masses of the gauge bosons

are generated from the infinite sum of iterations of coupled gauge boson and pseudo boson propagators, (i.e. 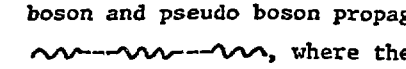 where the wave line is for the gauge boson propagator and dotted line for the dynamically generated pseudo scalar bosons.) Thus in this scheme of mass-generating, there is the by-product of many physical pseudo scalar bosons. The production of these technicolor pseudo scalar in hadronic scattering is mainly through the interaction gluon + gluon $\to q\bar{q} \to \pi'$, i.e. via a technicolor fermion loop. Their couplings to Z^o, i.e. $Z^o \to Z^o\pi'$, is extremely small as pointed out by Ref. (32) therefore the observation of a boson through the mechanism of bremsstrahlung from the Z^o will be a strong support of the elementary Higgs mass-generating mechanism.

III. e^+e^- INTERACTIONS AND COMPARISON WITH THE pp and $\bar{p}p$ INTERACTIONS

The corresponding production of Z^o, toponium and parity violation properties in the e^+e^- machine has been thoroughly reported in the previous Cornell study[6] and the LEP study.[7] The production rates of Z^o in e^+e^-, pp and $\bar{p}p$ machines are listed in Table I.

One important mechanism of producing the Higgs boson H^o in e^+e^- is via bremsstrahlung from the Z^o. In Fig. (3.1), (3.2) and (3.3) we show various distributions[33] of such a production of H^o. It is interesting to compare those in the pp and $\bar{p}p$ reactions, as given in Section II (E). In Table I, we also list the event rates. They are comparable for ISABELLE and the e^+e^- machine with their projected luminosity.

IV. SUMMARY

1. Because of the uniqueness of the production mechanism and absence of background, the e^+e^- machine can give a definite answer to the question on whether the predicted Z^o of 90 GeV exists or not.

2. For the same reason, if the Z^o is found, the e^+e^- machine provides a cleaner source of new flavors and the Higgs boson, if they exist. It is interesting to note that the event rates are about the same for bremsstrahlung production of H^o at the e^+e^- machine with 3×10^{31} $cm^{-2}sec^{-1}$ luminosity and the pp machine with 10^{33} $cm^{-2}sec^{-1}$ luminosity i.e. ISABELLE.

3. $W^{\pm}$ can only be effectively produced and searched for in pp and $\bar{p}p$ machines. The validity of the standard model can be checked only if the mass and parity properties of $W^{\pm}$ are also measured.

4. Due to the high energy of ISABELLE and the CERN $p\bar{p}$, Z^{o}'s and $W^{\pm}$'s of masses higher than predicted can also be sought.

5. In pp and $p\bar{p}$ new flavors can be more effectively produced via associative production, which is estimated to be an order of magnitude higher than from Z^{o} or $W^{\pm}$ decay.

6. Due to the complexity of nuclear matter, pp and $\bar{p}p$ machines in higher energies provide opportunities to produce new, unpredicted particles and phenomena.

We see that $e^{+}e^{-}$ and pp, $\bar{p}p$ machines play complementary roles. The advancement of our understanding depends on the success of both types of machines.

1. S. Weinberg, Phys. Rev. Lett 29, 388 (1972); J. C. Pati and A. Salam, Phys. Rev. D10, 275 (1974); R. N. Mohapatra and D. P. Sidhu, Phys. Rev. Lett. 38, 667 (1977); and BNL Report 22561 (1977) to be published in Phys. Rev. D; M. A. B. Beg, R. Budny, R. N. Mohapatra and A. Sirlin, Phys. Rev. Lett. 38, 1252 (1977); A. DeRujula, H. Georgi, S. L. Glashow, Harvard preprint (1977); G. Segre and J. Weyers, Phys. Rev. Lett. 65B, 243 (1977); P. Langacker and G. Segre, Phys. Rev. Lett. 39, 259 (1977); B. W. Lee and S. Weinberg, Phys. Rev. Lett. 38, 1237 (1977); F. Wilczeck, A. Zee and S. B. Treiman, Phys. Lett. 68B, 369 (1977); M. A. B. Beg, R. N. Mohapatra, A. Sirlin and H. S. Tsao, Rockefeller University Report COO-22328-133 (1977).

2. Talk by C. Baltay, Proceedings of the XIXth International Conference on High Energy Physics, Tokyo, August 1978.

3. J. C. Pati and A. Salam, Phys. Rev. Lett. 31, 661 (1973); Phys. Rev. D 8, 1240 (1973); H. Georgi and S. L. Glashow, Phys. Rev. Lett. 32, 438 (1974); H. Georgi, H. Quinn, S. Weinberg, Phys. Rev. Lett. 33, 451 (1974).

4. For a review, see M. Goldhaber, P. Langacker, R. Slansky, "Is the Proton Stable", Science, 210, 851 (1980).
For a review on future experiments measuring proton lifetime, see M. Goldhaber "Baryon Conservation (Experiments)", invited talk presented at the ν'80 Int. Conf. on ν-Physics and Astrophysics, Erice (Trapani), Italy, June 23-27, 1980.

5. See W. I. Marciano's talk at this workshop.

6. Design Study Proposal for A High Energy, High Luminosity Electron Positron Collider Based on Super Conducting RF Cavities, Cornell University, Ithaca, N.Y. 14853, May 1980

7. LEP Summer Study, des Houches and CERN, 10-22 Sept., 1978.

8. L.-L. Chau Wang, Theoretical Implications Of ISABELLE Physics, lecture delivered at the 1980 Erice Summer School.

9. L. B. Okun, Sov. J. Nucl. Phys. 3, 426 (1966); Y. Yamaguchi, Nuovo Cimento 43, 193 (1966).

10. ϕ: D. C. Hom et al., Phys. Rev. Lett. 37, 1374 (1976).
ϕ: D. C. Hom et al., Phys. Rev. Lett. 36, 1236 (1976).
ϕ: L. Kluberg et al., Phys. Rev. Lett. 37, 1451 (1976).
ϕ: M. Binkley et al., Phys. Rev. Lett. 37, 571 (1976).
ϕ: K. S. Anderson et al., Production of Continuum Muon Pairs at 225 GeV by Pions and Protons, Princeton preprint, July (1976).
ϕϕϕ: J. H. Christenson et al., Phys. Lett. 25, 1523 (1970); L. M. Lederman and B. G. Pope, Phys. Rev. Lett. 66B, 486 (1977).
Here the data with different longitudinal momentum acceptance were integrated by the Drell-Yan model. The lower energy data especially are rather sensitive to the Fermi motion correction.

11. ϕ D. Antreasyan et al., Phys. Rev. Lett. 45, 859 (1980).

12. C. Kourkoumelis et al., Phys. Lett. 91B, 475 (1980).

13. S. D. Drell and T.-M. Yan, Phys. Rev. Lett. 25, 316 (1970) and Ann. Phys. (N.Y.) 66, 578 (1971).

14. R. P. Feynman, Phys. Rev. Lett. 23, 1415 (1969); J. D. Bjorken and E. A. Paschos, Phys. Rev. 185, 1975 (1969).

15. D. J. Gross and F. A. Wilczek, Phys. Rev. Lett. 30, 1343 (1973); H. D. Politzer, ibid 30, 1346 (1973).

16. R. E. Taylor, Proc. 1975 Int. Symp. on Lepton and Photon Interactions at Highe Energies, Stanford, ed. by W. T. Kirk (Stanford Linear Accelerator Center, Stanford, 1975); Y. Watanabe et al., Phys. Rev. Lett. 35, 898, 901 (1975); H. L. Anderson et al., Phys. Rev. Lett. 37, 4 (1976) and 38, 1450 (1977); H. L. Anderson, H. S. Mathis and L. C. Myrianthopoulos, Phys. Rev. Lett. 40, 1061 (1978), and lecutres by D. H. Perkins and J. Ellis at the Summer Institute on Particle Physics, Weak Interactions - Present and Future, Stanford, CA, July 10-21, 1978).

17. See Review Talk by F. Sciulli, Proceedings of the XXth Int. Conf. on H.E. Physics July 17-23 1980, University of Wisconsin, Madison.

18. J. Kubar-Andre and F. E. Paige, Phys. Rev. D19, 221 (1979); G. Altarelli, R. K. Ellis, and G. Martinelli, Nucl. Phys. B157, 461 (1979).

19. R. F. Peierls, T. L. Trueman and L.-L. Wang, Phys. Rev. D16, 1397 (1977).

20. J. F. Owens and E. Reya, Phys. Rev. D17, 3003 (1978).

21. F. E. Paige "Updated Estimates of W Production in pp and $\bar{p}p$ Interactions" Proceedings of Topical Workshop on Production of New Particles in Super High Energy Collissions, Madison, Wisconsin (1979).

22. F. E. Paige, T. L. Trueman, T. N. Tudron, Phys. Rev. D19, 935 (1979).

23. T. L. Trueman (private communication).

24. T. K. Gaisser, F. Halzen and E. A. Paschos, Phys. Rev. D15, 2572 (1977).

25. C. Kourkoumelis et al., Phys. Lett. 91B, 481 (1980). For an earlier compilation, see M. Goldhaber and L.-L. Wang Phys. Rev. D18, 2364 (1978).

26. F. E. Paige, Private communication.

27. For a review on the current thinking on the Higgs boson see G. Barbiellini et al., DESY report 79/27 (1979) and talks by M. K. Gaillard, M. Veltman, Proceedings of the 1979 Int. Sym. on Lepton and Proton Interactions at High Energies.

28. For details see L. L. Chau Wang "Signature of the Bremsstrahlung of a Higgs Boson by Z^{o} in Hadronic Reactions", Brookhaven Preprint 1980.

29. For leptonic decay branching ratios for the τ and the b, see M. Perl, The Tau Lepton, SLAC preprint, SLAC-PUB-2446 (Dec. 1979), (submitted to Ann. Rev. Nucl. Part. Sci.). B. Gittelman's talk at the XXth Int. Conf. on High Energy Physics.

30. For review on the status of prompt lepton production, see talk by H. Wachsmuth, Proceedings of the 1979 Int. Sym. on Lepton and Photon Interactions at High Energies, Fermilab, Aug. 1979.
31. For a review on technicolor see M. A. B. Beg, Rockefeller University Report Number DOE/EY/2232B-211 (1980) (to appear in the Proceedings of the XXth Int. Conf. on High Energy Physics).
32. A. Ali and M. A. B. Beg, Production of Higgs Boson and Hyperpions in e^+e^- Annihilation, DESY and Rockefeller University
33. E. Ma and J. Okada, Phys. Rev. D20, 1052 (1979).

FIGURE CAPTIONS

Fig. (2.1a) Compilation of data $Q^3 \frac{d\sigma}{dQ}$ vs. s/Q^2, experiments with different longitudinal momentum acceptance are integrated according to the parton model used. Data are from Refs. (26), (27) and also Ref. (34). The dashed curves are the prediction of the Drell-Yan model using structure function of Ref. (35) which included the leading-log QCD corrections and the solid curve is calculated using the old structure function [See Ref. (34)].

Fig. (2.1b) Compilation of data $Q^3 \frac{d\sigma}{dQdy}\Big|_{y=0}$ vs. $Q/\sqrt{s}$, Ref. (28).

Fig. (2.2a) Diagram for the Drell-Yan model for hadronic inclusive production of the dilepton.

Fig. (2.2b) Diagram for the quark-parton model for lepton-hadron inelastic scattering.

Fig. (2.3a) Same as Fig. (2.2a), but includes loading-log gluon effects.

Fig. (2.3b) Same as Fig. (2.2b), but includes leading-log gluon effects.

Fig. (2.4a) Structure functions of electorn-hadron inelastic scattering, Ref. (32).

Fig. (2.4b) Structure functions including the perturbative QCD scaling violation effects, Ref. (32) and Ref. (35).

Fig. (2.5a) Total production cross section vs. $\sqrt{s}/m$ of W^- production for pp and $\bar{p}p$ scattering. Points indicate the production of W^- with mass m_W = 80 GeV at $\sqrt{s}$ = 800 GeV for pp scattering, and at $\sqrt{s}$ = 540 and 2000 GeV for $\bar{p}p$ scattering. Scale of event rates is

indicated on the right for luminosity = $10^{33}cm^{-2}sec^{-1}$, and a 3×10^7 sec year. See Ref. (36).

Fig. (2.5b) Same as Fig. (2.5a) but for Z^o with mass m_z = 90 GeV, Ref. (36).

Fig. (2.6) $\frac{d\sigma}{dQdy}\Big|_{y=0}$ for the dilepton of mass Q and rapidity $\bar{y}$ from a Z^o produced in pp (solid line) and in $\bar{p}p$ (dotted line). Event rates are also indicated for ISA with luminosity = $10^{33}cm^{-2}sec^{-1}$.

Fig. (2.7) $\frac{d\sigma}{dp\ d\Omega}\Big|_{\theta=90^o}$ for the e^+, with perpendicular momentum $P_\perp$ and solid angle Ω at $\theta=90^o$, from the decay of a W^+ produced in pp scattering at $\sqrt{s}$ = 800 GeV, Ref. (36). Event rate for luminosity = $10^{33}cm^{-2}sec^{-1}$ is also indicated.

Fig. (2.8) Distribution for pp→jet+jet+X at $\sqrt{s}$ = 800 GeV, for jet+jet from hadronic interactions (dotted line) and from W^+ decay (solid line), Ref. (37).

Fig. (2.9a), (2.9b) Angular distribution for e^+ (solid line) from W^+ and e^- (dotted line) from W^- produced in $p\bar{p}$ scattering at $\sqrt{s}$ = 540 GeV at various $P_\perp$ of the lepton as indicated. θ is the angle between the lepton and the incoming proton.

Fig. (2.9c), (2.9d) Same as Figs. (2.9a), (2.9b) but for pp scattering at $\sqrt{s}$ = 800 GeV.

Fig. (2.10a) Data compilations of scaling cross sections $\frac{M^3}{\Gamma_h}\frac{d\sigma}{dy}\Big|_{y=0}$ for the heavy vector bosons productions, Ref. (40).

Fig. (2.10b) Data compilation of the non-scaling cross sections $\frac{d\sigma}{dy}\Big|_{y=0}$ for the heavy vector boson productions, Ref. (40).

Fig. (2.11) Estimated production cross section $\frac{d\sigma}{dQdy}\Big|_{y=0}$ of heavy onia of mass Q in pp reaction with luminosity = $10^{33}cm^{-2}sec^{-1}$ at $\sqrt{s}$ = 800 GeV with a mass measurement resolution $\Delta Q/Q$ = 1%, see text, Ref. (41).

Fig. (2.12) Dilepton mass Q distribution for the bramsstrahlung of a H^o by a Z^o produced in $pp \to XZ^o \to XZ^oH^o \to X\ell\bar{\ell}H^o$ at $\sqrt{s}$ = 800 GeV, and Higgs boson mass m_H = 5, 10, 15, 20 GeV, and for $pp \to X(Z^o + \gamma_v) \to X\ell\bar{\ell}$ at the same energy Ref. (43).

Fig. (2.13) Same as Fig (5.1) but for m_H = 5 GeV, in pp scattering with $\sqrt{s}$ = 600, 800, 1000 GeV and in $\bar{p}p$ scattering with $\sqrt{s}$ = 540, 2000 Gev, Ref. (43).

Fig. (3.1) Total cross section for $e^+e^- \to \mu^+\mu^-H$ is plotted as a function of the total center-of-mass energy $\sqrt{s}$. The mass of the Higgs boson is taken to be 10 GeV.

Fig. (3.2) The differential cross section $d\sigma/dx$ for $e^+e^- \to \mu^+\mu^-H$ is plotted as a function of $x = m^2_{\mu\mu}/s$, at $\sqrt{s}$ = 90 GeV (solid curve) and at $\sqrt{s}$ = 110 GeV (dashed curve).

Fig. (3.3) The differential cross section $d\sigma'/dz$ for $e^+e^- \to \mu^+\mu^-$ + anything is plotted as a function of $z = m^2_{-}/s$, where m_{-} is the missing mass, at $\sqrt{s} = M_Z$ = 90 GeV. A cut of $x = m^2_{\mu\mu}/s > 0.5$ has been applied. The solid curve denotes the background contribution from τ, c, b, and t decay. The dashed curve represents a Higgs boson of 10 GeV with an experimental resolution of 1 GeV.

TABLE I.

	BNL ISABELLE	FERMILAB DOUBLER	CERN TEVATRON	CORNELL e^+e^-
$\sqrt{s}$ (GeV)	800	2000	540	100
L ($cm^{-2}sec^{-1}$)	10^{33}	10^{30}	10^{30}	3×10^{31}
Z^o ($\frac{events}{yr}$)	3×10^7	3×10^5	3×10^4	4×10^7
$W^{\pm}$ ($\frac{events}{yr}$)	6×10^7	3×10^5	6×10^4	
H^oZ^o $\hookrightarrow \ell\bar{\ell}$ ($\frac{events}{yr}$)	600	6	.6	800

yr $\equiv 3 \times 10^7$ sec

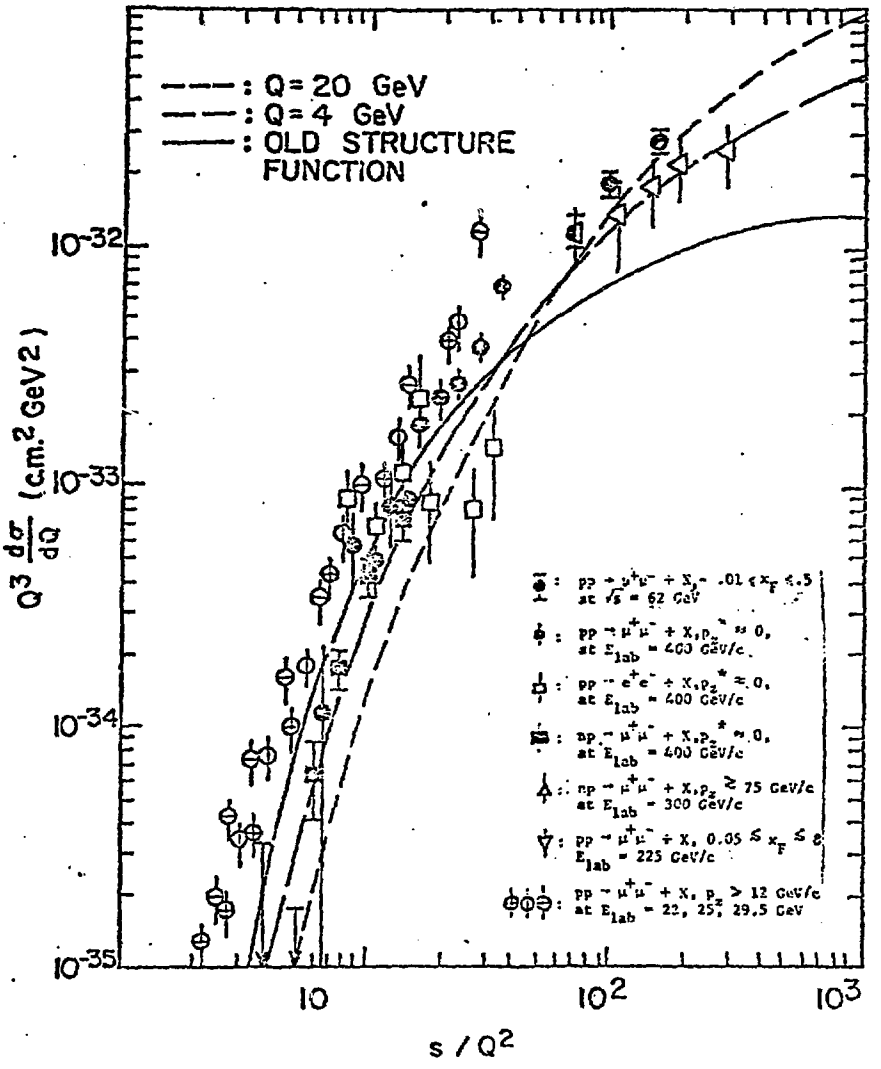
: Q = 20 GeV
: Q = 4 GeV
: OLD STRUCTURE FUNCTION
$Q^3 \frac{d\sigma}{dQ}$ (c.m.^{2} GeV2)
10^{-32}
10^{-33}
10^{-34}
10^{-35}
10
10^2
10^3
s / Q^2
$pp \to \mu^+\mu^- + X$, $-.01 < x_F < .5$ at $\sqrt{s}$ = 62 GeV
$pp \to \mu^+\mu^- + X, p_z^* \approx 0$, at E_{lab} = 400 GeV/c
$pp \to e^+e^- + X, p_z^* \approx 0$, at E_{lab} = 400 GeV/c
$pp \to \mu^+\mu^- + X, p_z^* \approx 0$, at E_{lab} = 400 GeV/c
$pp \to \mu^+\mu^- + X, p_z \geq 75$ GeV/c at E_{lab} = 300 GeV/c
$pp \to \mu^+\mu^- + X$, $0.05 \leq x_F \leq$ at E_{lab} = 225 GeV/c
$pp \to \mu^+\mu^- + X$, $p_z > 12$ GeV/c at E_{lab} = 22, 25, 29.5 GeV

Fig. (2.1a)

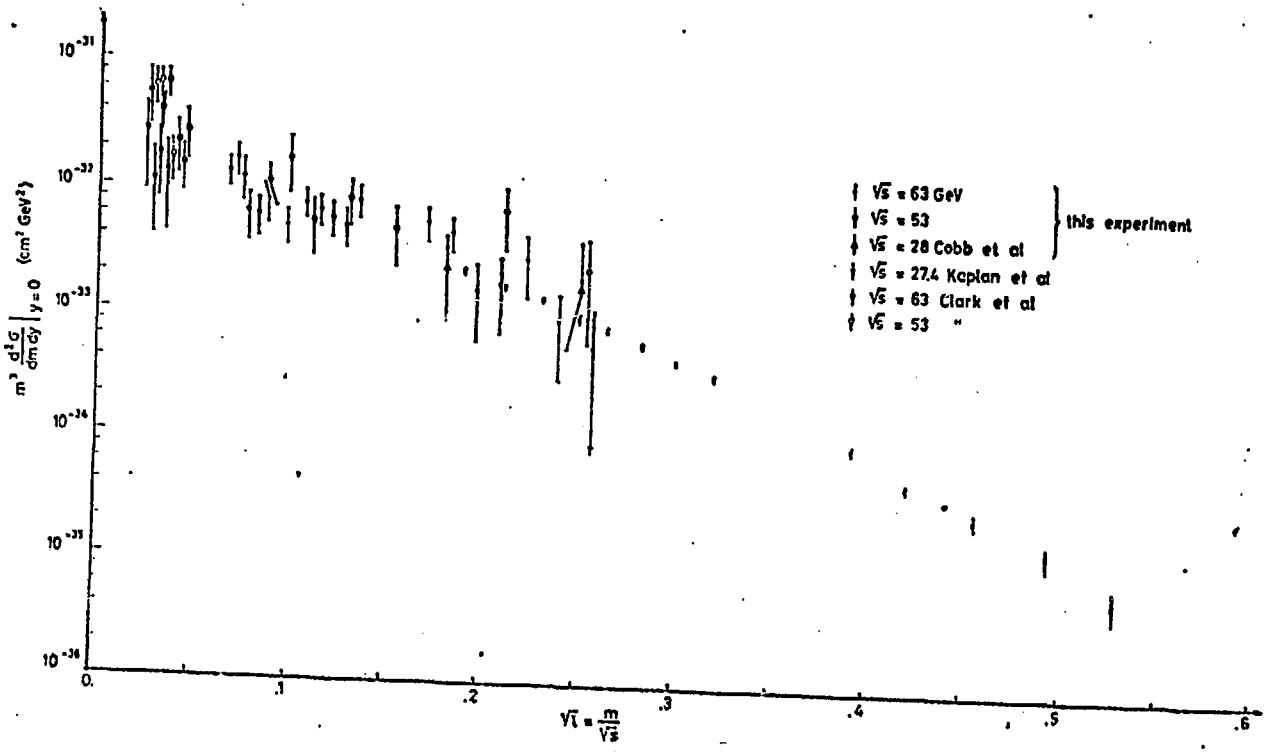
$m^3 \frac{d^2\sigma}{dm\,dy}\Big|_{y=0}$ (cm² GeV⁻²)
10^{-31}
10^{-32}
10^{-33}
10^{-34}
10^{-35}
10^{-36}
0.
.1
.2
.3
.4
.5
.6
$\sqrt{\tau} = \frac{m}{\sqrt{s}}$
$\sqrt{s}$ = 63 GeV
$\sqrt{s}$ = 53
$\sqrt{s}$ = 28 Cobb et al
$\sqrt{s}$ = 27.4 Kaplan et al
$\sqrt{s}$ = 63 Clark et al
$\sqrt{s}$ = 53 "
this experiment

Fig. (2.1b)

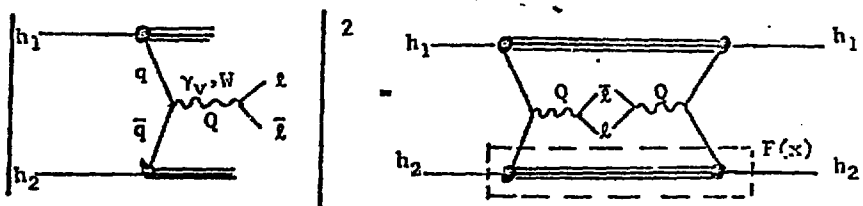

Fig.(2.3a)

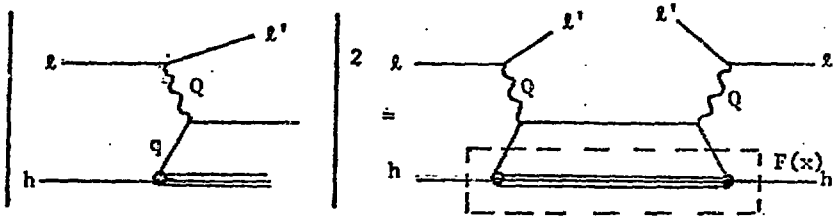

Fig.(2.3b)

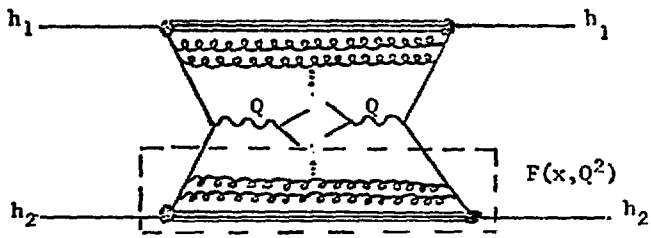

Fig.(2.4a)

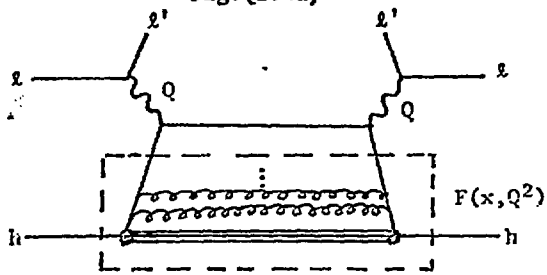

Fig.(2.4b)

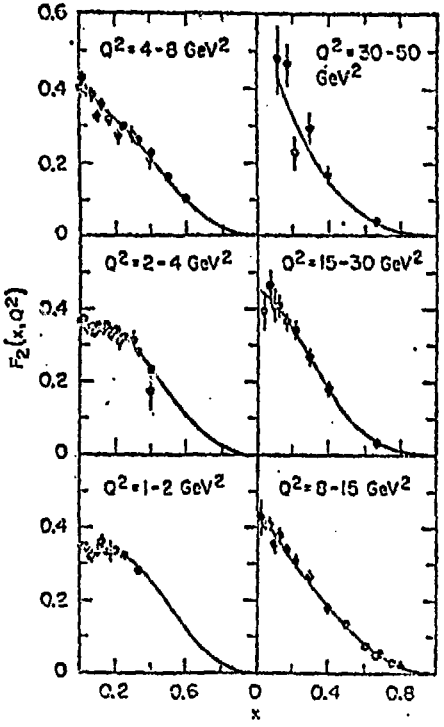

Fig. (2.4a)

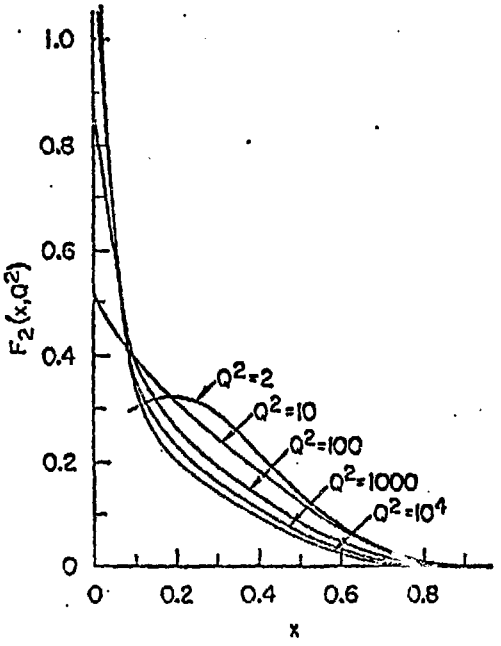

Fig. (2.4b)

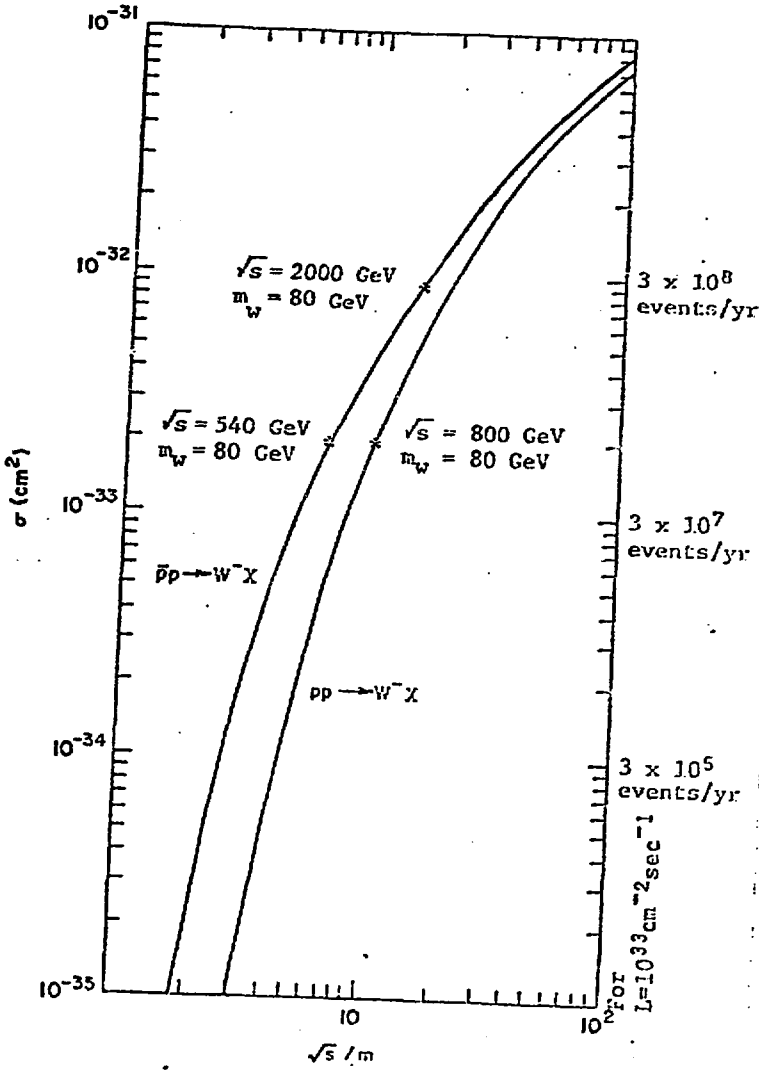
10^{-31}
10^{-32}
10^{-33}
10^{-34}
10^{-35}
σ (cm^2)
$\sqrt{s}$ = 2000 GeV
m_W = 80 GeV
$\sqrt{s}$ = 540 GeV
m_W = 80 GeV
$\sqrt{s}$ = 800 GeV
m_W = 80 GeV
$\bar{p}p \rightarrow W^- X$
$pp \rightarrow W^- X$
3 x 10^8 events/yr
3 x 10^7 events/yr
3 x 10^5 events/yr
For $L=10^{33} cm^{-2} sec^{-1}$
10
10^2
$\sqrt{s}$ / m

Fig. (2.5a)

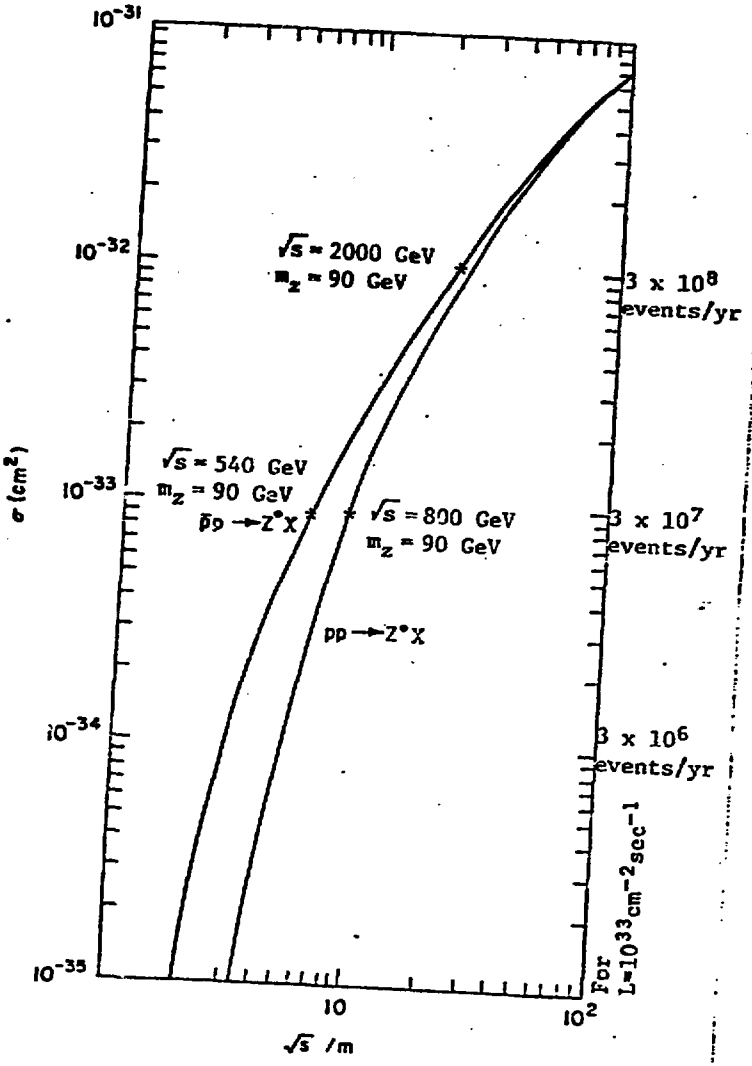
10^{-31}
10^{-32}
10^{-33}
10^{-34}
10^{-35}
σ (cm^2)
$\sqrt{s}$ = 2000 GeV
m_z = 90 GeV
$\sqrt{s}$ = 540 GeV
m_z = 90 GeV
$\bar{p}p \rightarrow Z^\circ X$
$\sqrt{s}$ = 800 GeV
m_z = 90 GeV
$pp \rightarrow Z^\circ X$
3 x 10^8 events/yr
3 x 10^7 events/yr
3 x 10^6 events/yr
For $L=10^{33} cm^{-2} sec^{-1}$
10
10^2
$\sqrt{s}$ /m

Fig. (2.5b)

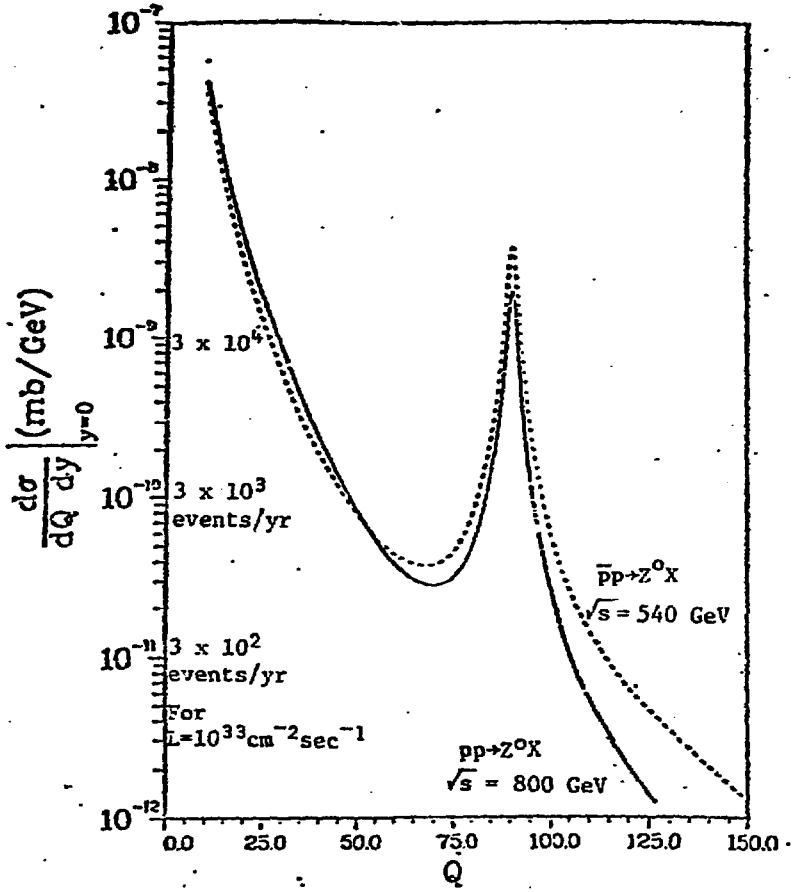
10^{-7}
10^{-9}
10^{-11}
10^{-13}
10^{-15}
10^{-12}
$\frac{d\sigma}{dQ\,dy}\Big|_{y=0}$ (mb/GeV)
3 x 10^4
3 x 10^3 events/yr
3 x 10^2 events/yr
For L=10^{33}cm^{-2}sec^{-1}
$\bar{p}p \to Z^0X$
$\sqrt{s}$ = 540 GeV
$pp \to Z^0X$
$\sqrt{s}$ = 800 GeV
0.0
25.0
50.0
75.0
100.0
125.0
150.0
Q

Fig. (2.6)

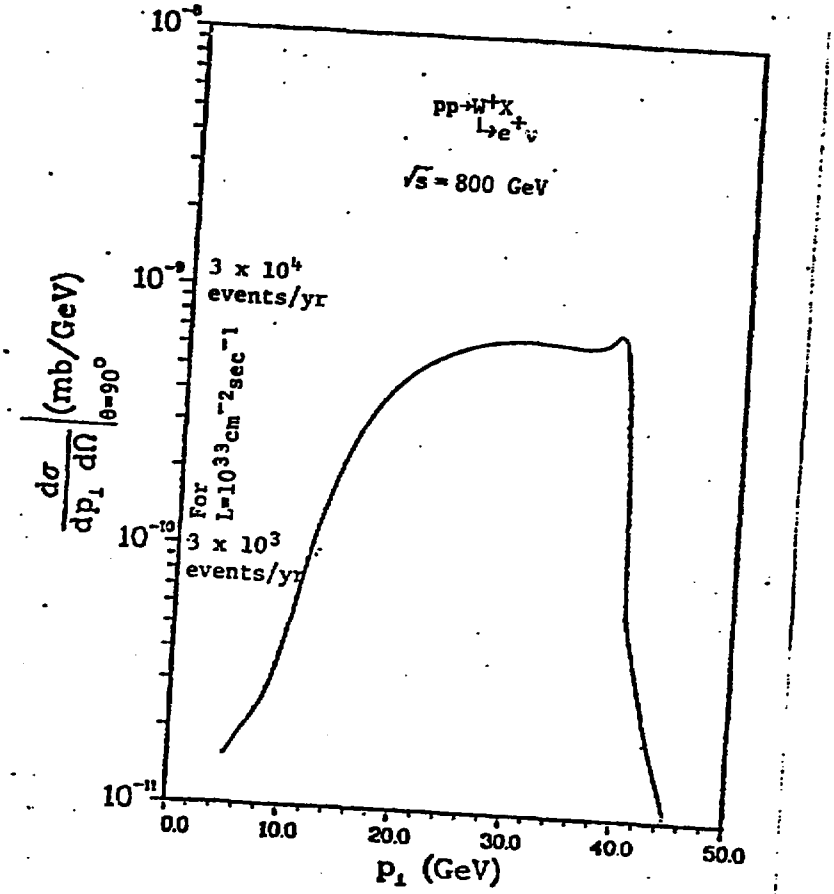
10^{-8}
10^{-9}
10^{-10}
10^{-11}
$pp \to W^{\pm} X$
$L \to e^{\pm} \nu$
$\sqrt{s} = 800$ GeV
3 x 10^4 events/yr
For $L = 10^{33} cm^{-2} sec^{-1}$
3 x 10^3 events/yr
$\frac{d\sigma}{dp_\perp d\Omega}\Big|_{\theta=90^\circ}$ (mb/GeV)
0.0
10.0
20.0
30.0
40.0
50.0
$p_\perp$ (GeV)

Fig. (2.7)

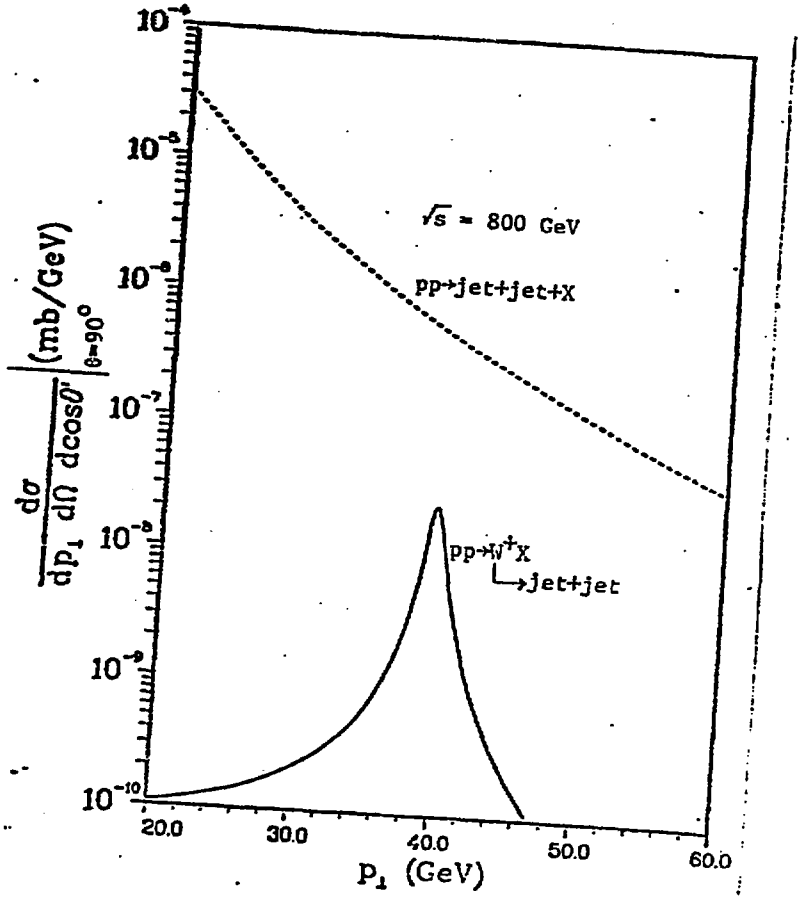
$\frac{d\sigma}{dp_\perp\, d\Omega\, d\cos\theta'}\Big|_{\theta=90^\circ}$ (mb/GeV)
10^{-4}
10^{-6}
10^{-8}
10^{-2}
10^{-6}
10^{-8}
10^{-10}
$\sqrt{s}$ = 800 GeV
pp→jet+jet+X
pp→W$^+$X
↳jet+jet
20.0
30.0
40.0
50.0
60.0
$P_\perp$ (GeV)

Fig. (2.8)

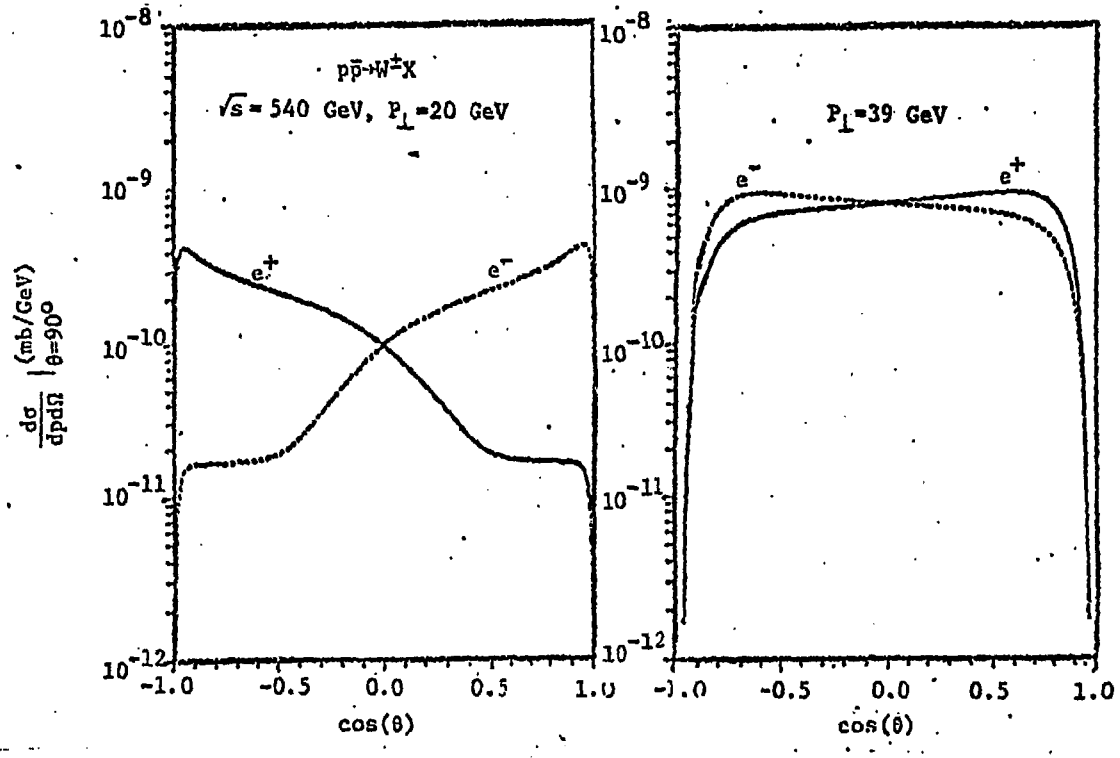

Fig. (2.9a)

Fig. (2.9b)

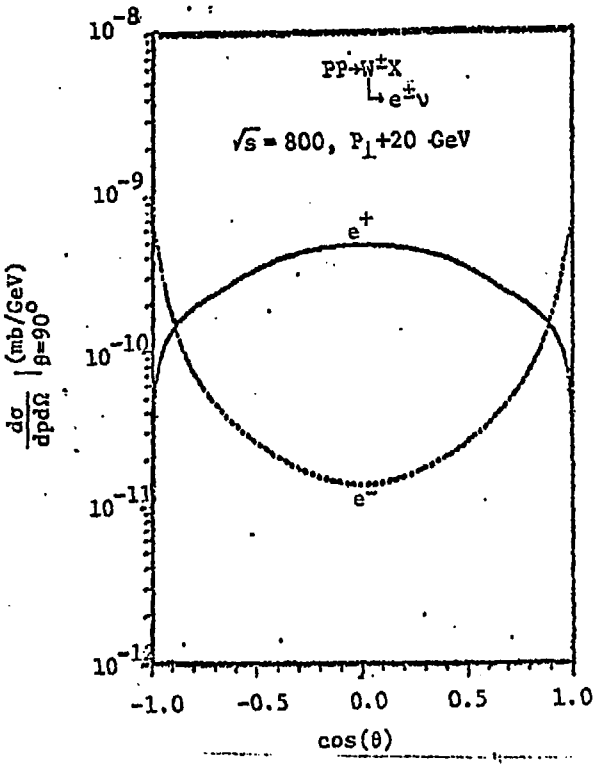

Fig. (2.9c)

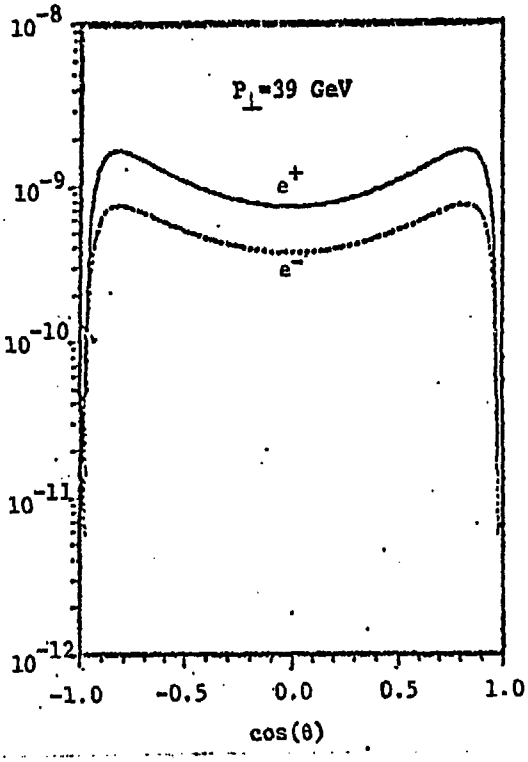

Fig. (2.9d)

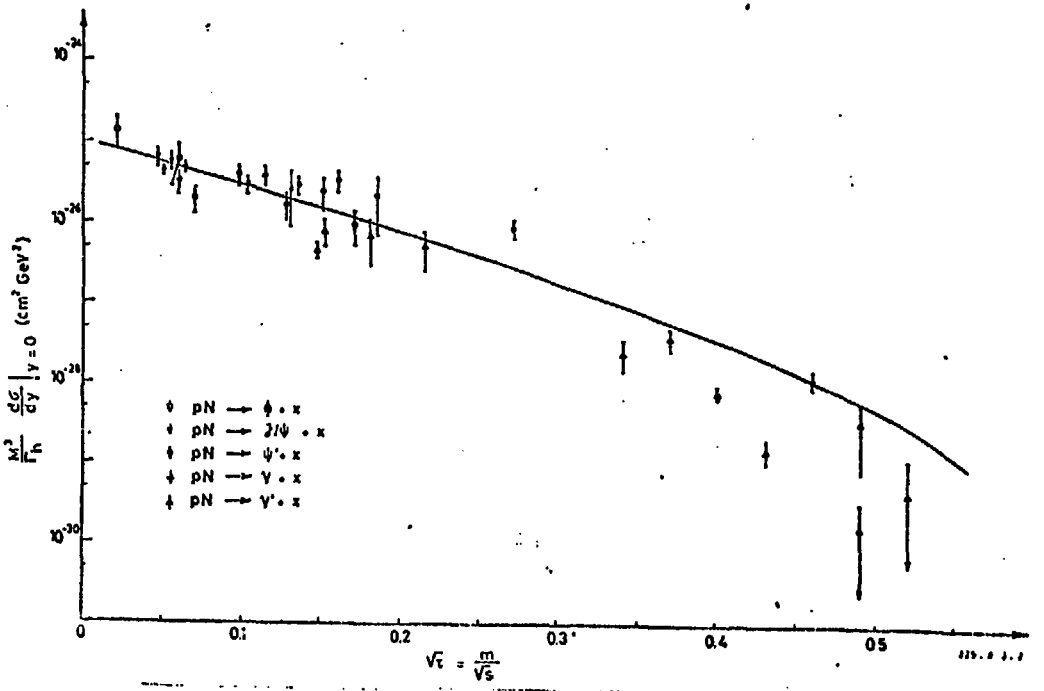

Fig. (2.10a)

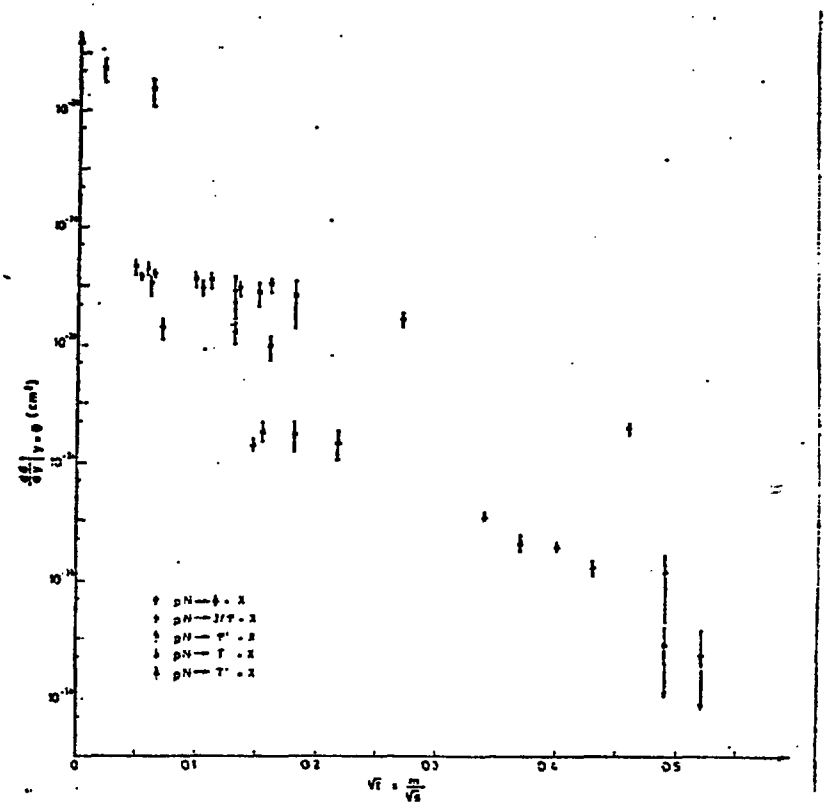

Fig. (2.10b)

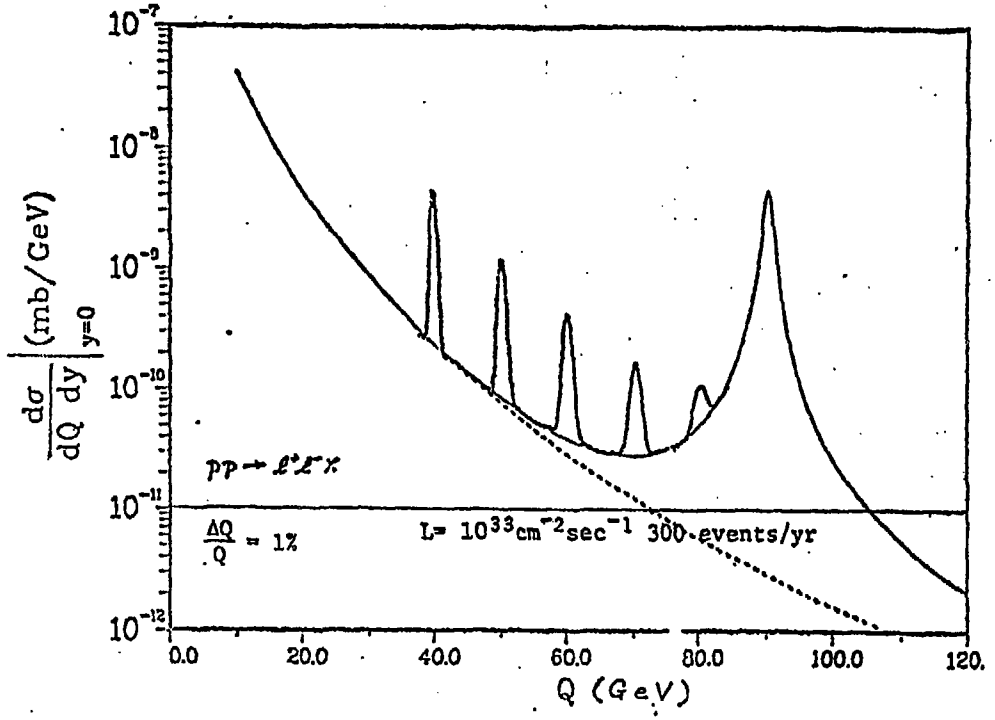
10^{-7}
10^{-8}
10^{-9}
10^{-10}
10^{-11}
10^{-12}
$\frac{d\sigma}{dQ\ dy}\Big|_{y=0}$ (mb/GeV)
$pp \to \ell^+\ell^- X$
$\frac{\Delta Q}{Q} = 1\%$
L= $10^{33}cm^{-2}sec^{-1}$ 300 events/yr
0.0
20.0
40.0
60.0
80.0
100.0
120.
Q (GeV)

Fig. (2.11)

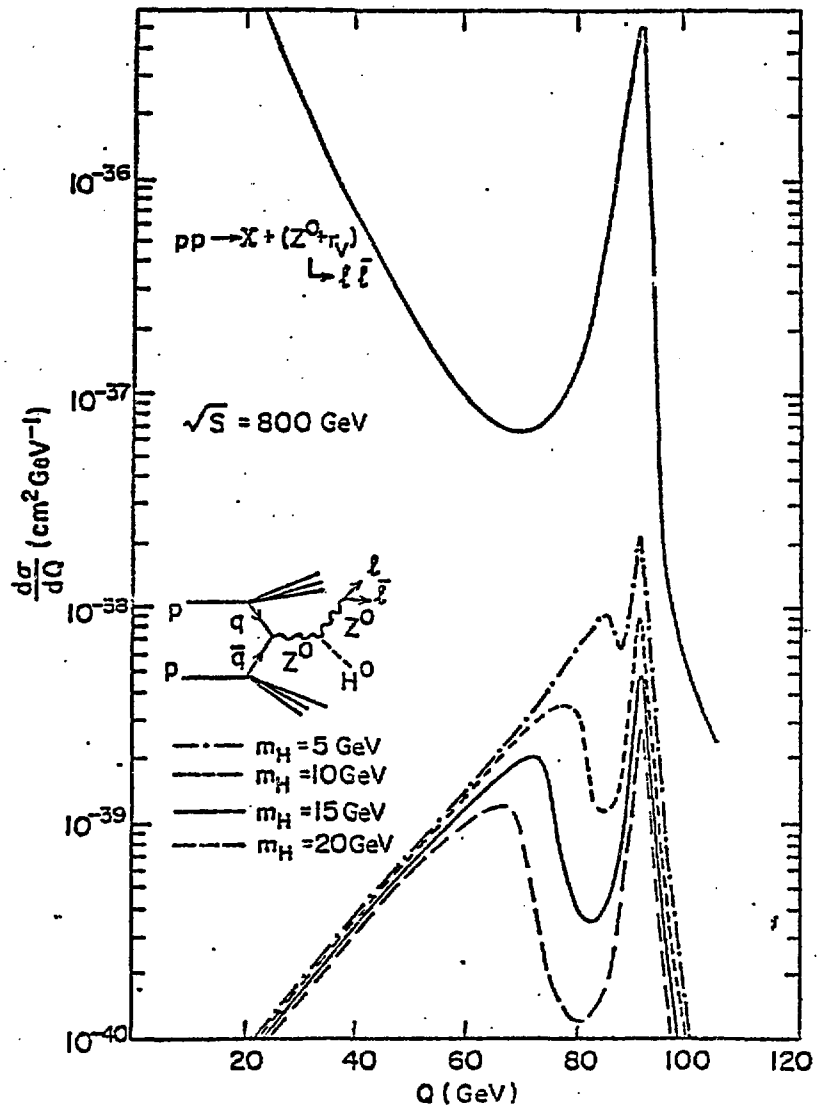
10^{-36}
10^{-37}
10^{-38}
10^{-39}
10^{-40}
$\frac{d\sigma}{dQ}$ (cm^{2}GeV^{-1})
$pp \to X + (Z^0 + \gamma_V)$
$\hookrightarrow l\bar{l}$
$\sqrt{s}$ = 800 GeV
p
q
$\bar{q}$
p
Z^0
Z^0
H^0
l
$\bar{l}$
m_H = 5 GeV
m_H = 10 GeV
m_H = 15 GeV
m_H = 20 GeV
20
40
60
80
100
120
Q (GeV)

Fig. (2.12)

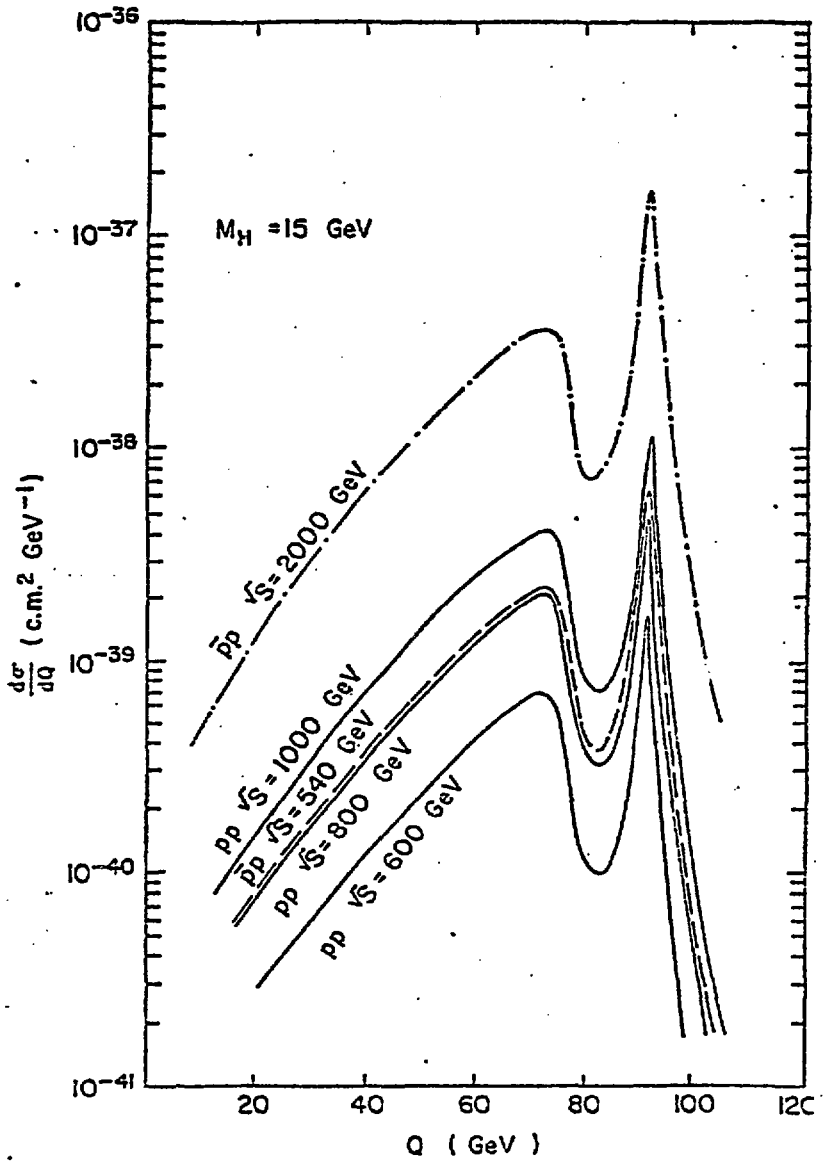
10^{-36}
10^{-37}
10^{-38}
10^{-39}
10^{-40}
10^{-41}
$\frac{d\sigma}{dQ}$ (c.m.^{2} GeV^{-1})
M_H =15 GeV
$\bar{p}p$ $\sqrt{S}$=2000 GeV
pp $\sqrt{S}$=1000 GeV
$\bar{p}p$ $\sqrt{S}$=540 GeV
pp $\sqrt{S}$=800 GeV
pp $\sqrt{S}$=600 GeV
20
40
60
80
100
120
Q (GeV)

Fig. (2.13)

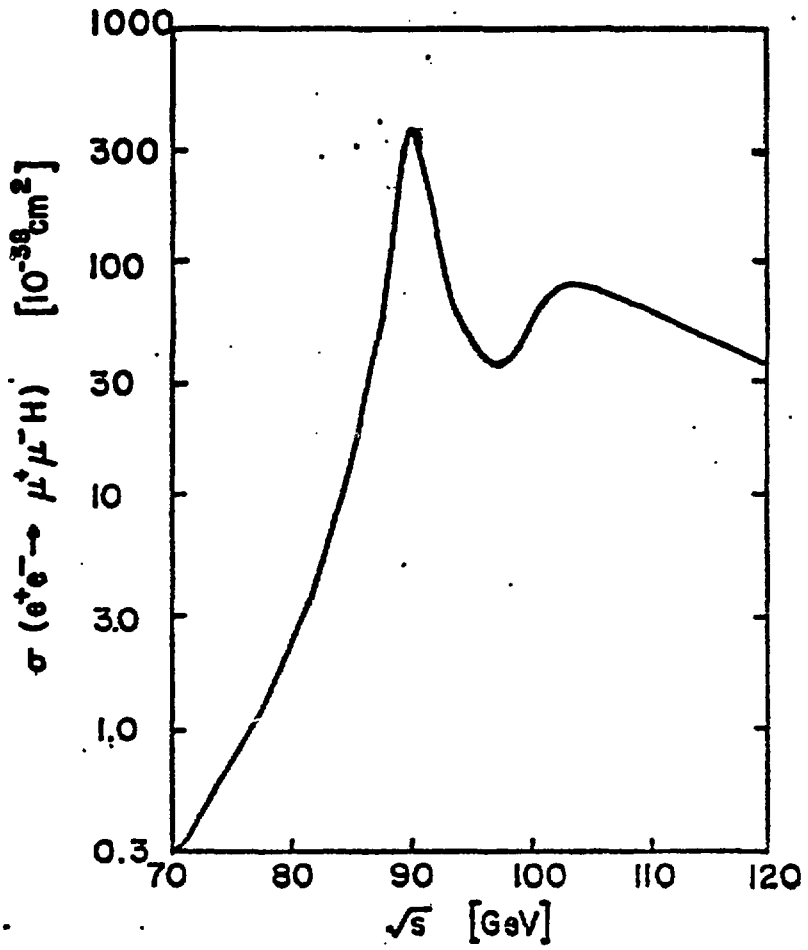
1000
300
100
30
10
3.0
1.0
0.3
70
80
90
100
110
120
√s [GeV]
σ (e⁺e⁻ → μ⁺μ⁻H) [10⁻³⁹cm²]

Fig. (3.1)

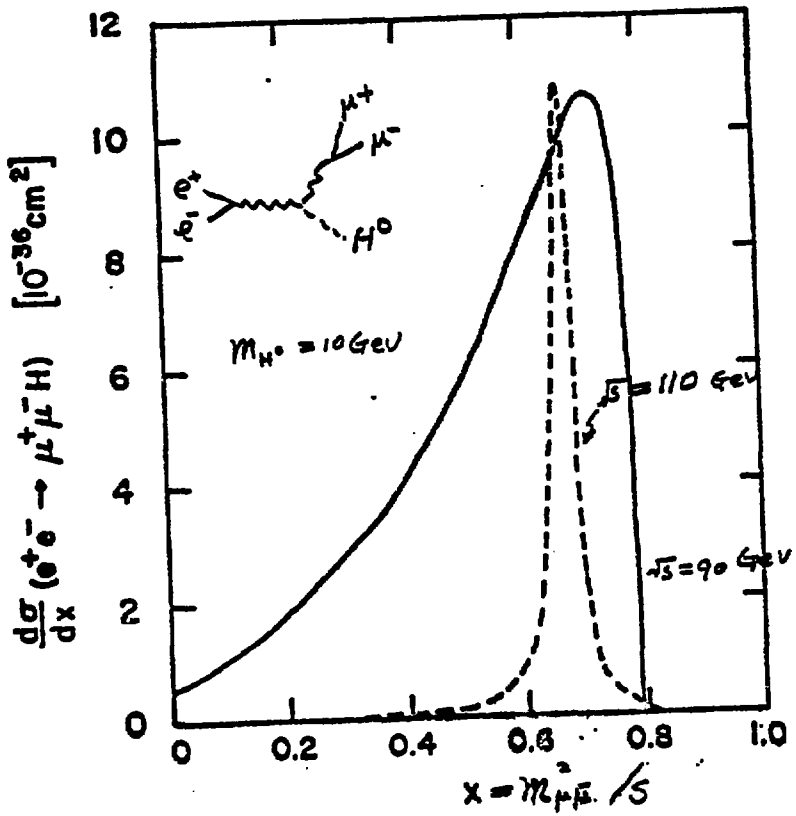
12
10
8
6
4
2
0
0
0.2
0.4
0.6
0.8
1.0
$\frac{d\sigma}{dx}(e^+e^- \to \mu^+\mu^- H)$ [10^{-36}cm^2]
$x = m^2_{\mu\mu}/s$
μ^+
μ^-
e^+
e^-
H^0
$m_{H^0} = 10$ GeV
$\sqrt{s} = 110$ GeV
$\sqrt{s} = 90$ GeV

Fig. (3.2)

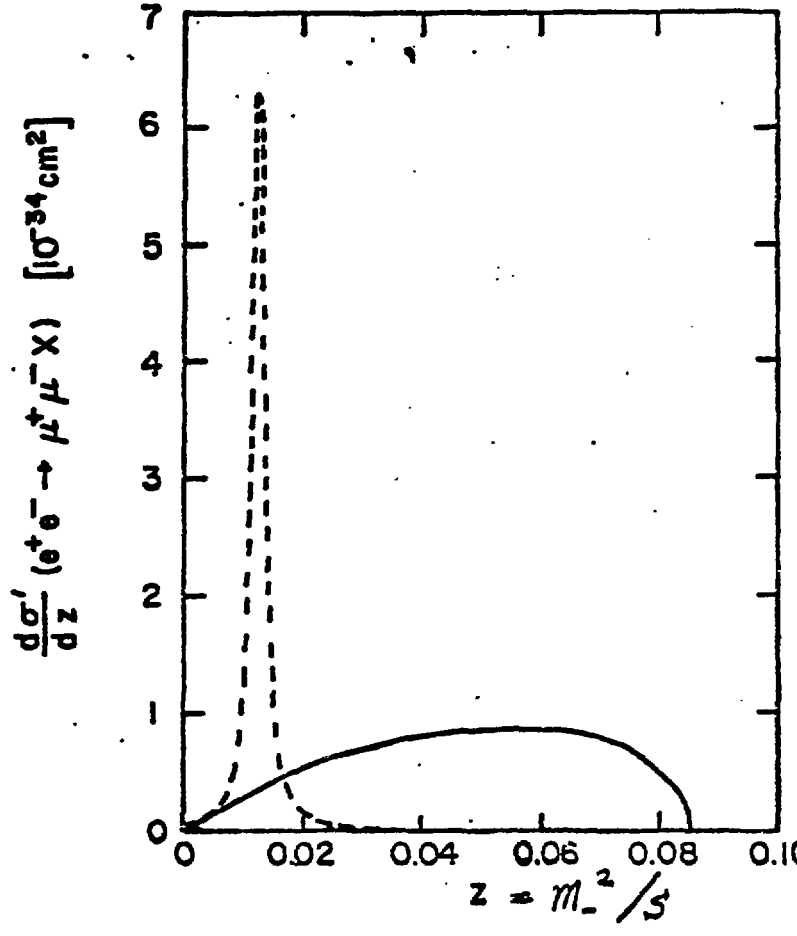
$\frac{d\sigma'}{dz}(e^+e^- \to \mu^+\mu^- X)$ $[10^{-34}cm^2]$
7
6
5
4
3
2
1
0
0
0.02
0.04
0.06
0.08
0.10
$z = m_-^2/s$

Fig. (3.3)